Nuclear Engineering and Technology 51 (2019) 1835–1841

Contents lists available at ScienceDirect

Nuclear Engineering and Technology

journal homepage: www.elsevier.com/locate/net

Original Article

Gamma ray shielding characteristics and exposure buildup factor for some natural rocks using MCNP-5 code

K.A. Mahmoud [a, b, *], M.I. Sayyed [c], O.L. Tashlykov [a]

[a] Ural Federal University, St. Mira, 19, 620002, Yekaterinburg, Russia
[b] Nuclear Materials Authority, Maadi, Cairo, Egypt
[c] Physics Department, University of Tabuk, Tabuk, Saudi Arabia

ARTICLE INFO

Article history:
Received 24 April 2019
Received in revised form
7 May 2019
Accepted 14 May 2019
Available online 17 May 2019

Keywords:
Gamma ray
Shielding properties
Natural rocks
MCNP
Buildup factor

ABSTRACT

The mass attenuation coefficient μ_m for eight rock samples having different chemical composition was simulated using the MCNP 5 code in energy range ($0.002MeV \leq E \leq 10$ MeV). Moreover, the μ_m for the studied rock samples was computed theoretically using XCOM database. The comparison between simulated and computed data for all selected rock samples showed a good agreement with differences varied between 0.01 and 8%. The highest μ_m was found for basalt rocks M2 and M1 and the lowest one is reported for limestone rocks Dike. The simulated values of the μ_m then were used to calculate other important shielding parameters such as the mean free path, effective electron density and effective atomic number. The exposure buildup factor EBF was also computed for the selected rocks with the contribution of G-P fitting parameters and the highest EBF attended by the basalt sample Sill and varied between 1.022 and 744 in the energy range between ($0.015 \leq E \leq 15$ MeV) but the lowest EBF achieved by basalt sample M2 and varied between 1.017 and 491 in the same energy range.

1. Introduction

Nowadays, nuclear power and solar energy become alternative sources due to the limitation of the natural fossil fuel resources. Gamma ray emitted from the nuclear power stations can travel for several Kilometers in the surrounding medium due to its high penetrating power [1,2]. These gamma photons cause indirectly ionizing for the water molecules in the human cells, which have a dangerous effects on the human DNA [1–3]. Therefore, a great attention has been given to the shielding properties evaluation of the various materials.

In the last few years, the researchers and investigators reported a great number of articles, which aimed to evaluate the shielding properties of different materials such as rocks [4,5], concretes [2,6–8], building materials [9,10], ceramics [11] alloys [12–14] nanocomposites [15], polymers [16] and glasses [17–22].

In practical applications, concrete is considered as one of the most materials utilized for radiation shielding aims. It can be formed into any required size and shape and it is composition can be changed easily according to the need. Some type of concretes especially the heavy concretes are very costly and therefore are important to find other materials that can be used as alternative materials in different shielding applications.

Rocks are usually used as building materials in several constructions, household tiles, hospitals, schools, universities and other facilities. For this reason, it is considerable to evaluate the response of the rocks to gamma radiations.

The natural rocks are cheap, available and uniform in composition and effective materials which can be used directly for radiation shielding purposes or used as aggregates in different concretes. Eight different natural samples of basalt (Sill), basalt bomb (M1 and M2), Rhyolite (AG) and limestone with different formation (Dike, M3, M4, M5) were investigated in this study.

In the present work, the mass attenuation coefficient μ_m is simulated for different rock samples collected from south western Sinai, Egypt using the MCNP 5 code Besides, other shielding parameters which describe the diffusion and penetration of incident gamma ray on the selected rocks are calculated. Moreover, the equivalent atomic number Z_{eq} and exposure buildup factor (EBF) are computed for the selected rock samples in energy range ($0.015 < E < 15$ MeV).

* Corresponding author. Ural Federal University, St. Mira, 19, 620002, Yekaterinburg, Russia.
E-mail addresses: kmakhmud@urfu.ru, karemabdekazeem@yahoo.com (K.A. Mahmoud).

https://doi.org/10.1016/j.net.2019.05.013

Table 1
The fractional abundance of elements in the rock samples.

Sample	Density (g/cm3)	Fractional abundance (%)										
		O	Na	Mg	Al	Si	P	K	Ca	Ti	Cr	Fe
AG	2.570	49,5	0.22	0,59	0.29	38,5	0.52	0,08	0.85	0.08	0.85	8,65
Dike	1.751	0.13	8.84	51.12	1.01	1.91	0.48	19.21	0.20	0.07	12.89	0.43
Sill	2.375	0.27	0.15	29.74	1.62	3.94	5.57	42.77	0.23	1.15	6.63	0.65
M1	2.464	0.30	0.25	30.26	2.75	3.76	5.31	38.86	0.23	1.08	6.82	0.95
M2	2.449	0.36	0.29	30.87	2.81	3.81	5.42	37.97	0.22	1.04	6.97	0.95
M3	2.011	0.30	2.97	35.95	0.12	4.90	0.87	39.98	0.23	0.11	10.83	0.35
M4	1.624	0.62	6.04	46.78	0.13	3.39	0.94	21.65	0.37	0.33	18.96	0.03
M5	1.60	0.59	5.40	44.38	0.06	1.45	0.40	22.82	0.40	0.27	23.97	0.01

2. Material and methods

2.1. Shielding parameters

In the present work, the probability in which the incident gamma ray beam of photons with intensity $I_\circ$ interact with a slide of natural rock with thickness x (cm) is defined as the gamma ray linear attenuation coefficient (μ), which described by Beer's law namely (1) [23]:

$$\mu\left(cm^{-1}\right) = \frac{1}{x}\ln\left(\frac{I_o}{I}\right) \quad (1)$$

The mass attenuation coefficient (μ_m) for a given material is considered as an important shielding parameter. It is used to characterize and describe the gamma ray penetration and interaction with the rock slides. The experimental and theoretical calculations of the μ_m for a given material can described by equations (2) and (3) respectively [24].

$$\mu_m\left(cm^2.\,g^{-1}\right) = \frac{\mu\left(cm^{-1}\right)}{\rho\left(g.cm^{-3}\right)} \quad (2)$$

$$\mu_m\left(cm^2.g^{-1}\right) = \sum_i (\mu_m)_i.\omega_i \quad (3)$$

Where ρ is the studied material density, ω_i is the weight fraction of the i^{th} constituent element and $(\mu_m)_i$ is the total attenuation coefficient for the i^{th} constituent element in the rock samples.

During the interaction of gamma ray with the rock samples, the distance between two following collisions is defined as the Mean free path (MFP) and described by equation (4), [25].

$$MFP\ (cm) = \frac{1}{\mu\left(cm^{-1}\right)} \quad (4)$$

Moreover, the atomic cross sections (σ_a) and electric cross sections (σ_e) were calculated according to equations (5) and (6) respectively [26,27].

$$\sigma_a = \frac{1}{N_A}\sum f_i A_i (\mu_m)_i \quad (5)$$

$$\sigma_e = \frac{1}{N_A}\sum \frac{f_i A_i}{Z_i}(\mu_m)_i \quad (6)$$

Where f_i denotes the fractional abundance for the i^{th} constituent element. It is important to state that the chemical composition of the studied rock samples was analyzed utilizing induced coupling plasma optical emission spectroscopy (ICP-OES) [28] and the composition of the rocks under investigation is tabulated in Table 1. A_i and Z_i are respectively the mass number and the atomic number of the i^{th} constituent element.

The effective atomic number and effective electron density for the studied rock samples were derived using the calculated (σ_a) and (σ_e) according to equations (7) and (8) [27,29].

$$Z_{eff} = \frac{\sigma_a}{\sigma_e} \quad (7)$$

$$N_{eff} = \frac{N_A}{M} Z_{eff} \sum n_i \quad (8)$$

Where M is the atomic mass of the material.

Exposure building up factor (EBF) is an important factor used to correct the attenuation calculation. Moreover, the EBF can be computed for the selected rock samples with the help of Geometric-progress (G-P) fitting equations [30–32] Calculation of the EBF was achieved throughout three following steps reported as the following:

i) Calculation of the equivalent atomic number (Z_{eq}) which is a quantity described shielding features of the studied rock samples in term of its equivalent elements and defined by equation (9).

$$Z_{eq} = \frac{Z_1(\log R_2 - \log R) + Z_2(\log R - \log R_1)}{(\log R_2 - \text{Log } R_1)} \quad (9)$$

In the previous equation R_1 and R_2 are the ratios of $\left(\mu_{comp}/\mu_{total}\right)$ corresponding to elements with atomic number Z_1 and Z_2.

ii) Calculation of Geometric-progress fitting parameters such as (b, a, X_k, x and c) with the help of the ANSI/ANS-6.4.3 standard database [33] using the interpolation equation (10).

$$C = \frac{C_1\left(\log Z_2 - \log Z_{eff}\right) + C_2\left(\log Z_{eff} - \log Z_1\right)}{(\log Z_2 - \text{Log } Z_1)} \quad (10)$$

Where C_1 and C_2 denote the G-P fitting parameters obtained from the standard database for Z_1 and Z_2 respectively.

iii) The EBF values for the rock samples were calculated in energy range between 0.015 and 15 MeV with the help of calculated G-P fitting parameters as shown in equations (11)–(13).

$$B(E,x) = 1 + \frac{(bC-1)}{(K-1)}(K^x - 1), K \neq 1 \quad (11)$$

$$B(E,x) = 1 + (b-1)x,\ K = 1 \quad (12)$$

$$K(E,x) = cx^{a} + d\frac{\tanh\left(\frac{x}{X_k} - 2\right) - \tanh(-2)}{1 - \tanh(-2)},\ x \leq 40\ \text{mfp} \quad (13)$$

Where x is the distance between the monoenergetic source and the detector in term of mfp, and b is the EBF value when the distance between the source and detector equal to 1mfp.

2.2. MCNP simulation

Monte Carlo N particle transport code (MCNP 5) code is a program for modeling the interaction of neutrons, gamma and X rays and electrons in different materials. The MCNP-5 code uses the nuclear cross section libraries and different physics models for the particle interactions with the matter. The simulated parameters using MCNP have a very low error percent around 1% [17]. MCNP simulation of the gamma ray shielding parameters for different rock samples requires information about the geometry, the rocks chemical composition and densities, source and tally specification. The geometry used in the present work is shown in Fig. 1 and it is considered as an evacuated cylinder made of lead with diameter 25 cm, height 30 cm and thickness 5 cm. The environment for the mentioned cylinder was filled with air; a cylindrical collimator of lead was placed at the center of the problem geometry with a slit 5 cm. Finally, a mono energetic source placed inside the collimator at a distance 5 cm from the rock samples and 15 cm from the detector which considered as F4 tally in this work. The NPS variable (History cutoff card) was set to be 1000000 tracked particles. The results were reported with error about 1%.

2.3. XCOM calculation

XCOM is a database created by created by Berger and Hubell in 1987 to calculate mass attenuation coefficient of elements, compounds and mixtures in energy range between (1 KeV < E < 1 GeV) [34]. Many articles were reported using XCOM database for the mass attenuation coefficient calculation in different mixtures such as building materials [35], polymers [36–38], glasses [39] and concretes [40]. In the present work XCOM database was used to validate the simulated μ_m values for the studied rock samples. The different rock samples were identified for the XCOM program through their chemical composition. Then we compared the obtained μ_m results with those simulated by MCNP5 in order to check the accuracy in the input file.

3. Results and discussion

The μ_m of eight different rock samples collected from south western Sinai, Egypt was simulated using MCNP 5 code at energy range varied between 0.001 MeV and 10 MeV. The manner in which the μ_m for the selected rocks varied with the incident gamma ray energy was illustrated Fig. 2. It is clear that the μ_m for all selected rocks tend to maximum values (in the range of 1147–2125cm^2 /g for Dike and AG respectively) at gamma ray energy 0.002 MeV. Firstly, at a low gamma ray energy range between 0.002 and 0.02 MeV the μ_m for all rock samples decreased rapidly with increase the gamma energy. The rapid decrease in the μ_m of the selected rocks is resulting due to the absorption photoelectric which is dominated in the low energy region ($\sigma_{photoele} \propto Z^n.E^{-3.5}$, $n = 4-5$) [7,41]. The highest μ_m in low energy region attended by AG rock sample and varied between 2125 cm^2 /g (at 0.002 MeV) and 5 cm^2 /g at (0.02 MeV), but the lower μ_m was attended by Dike and varied

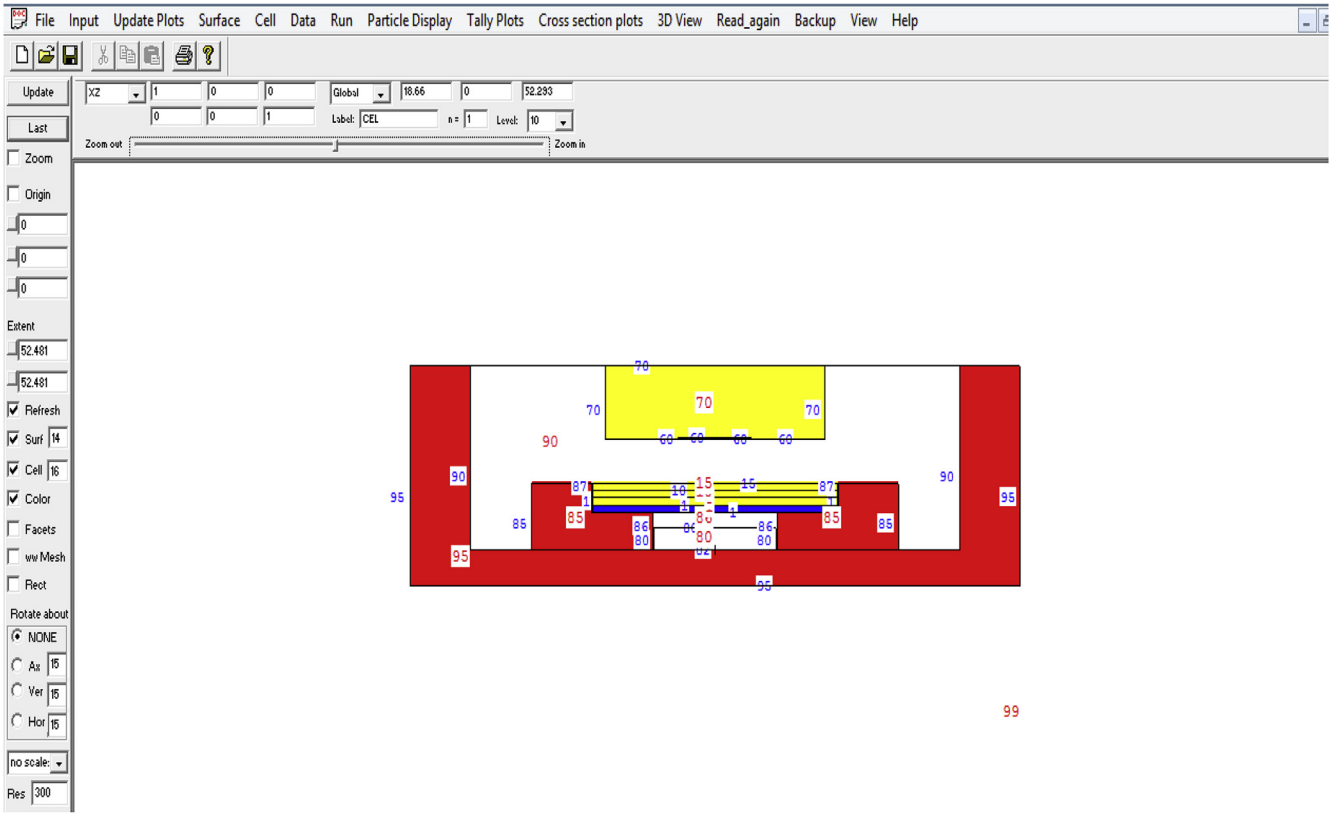

Fig. 1. The geometry used for simulation study.

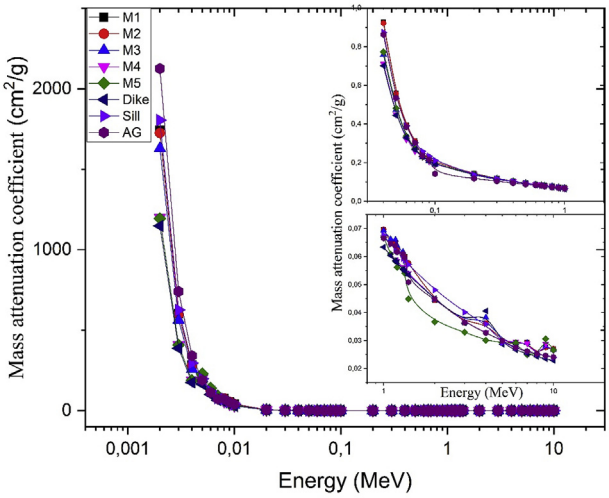

Fig. 2. The variation of the mass attenuation coefficient with gamma ray energy.

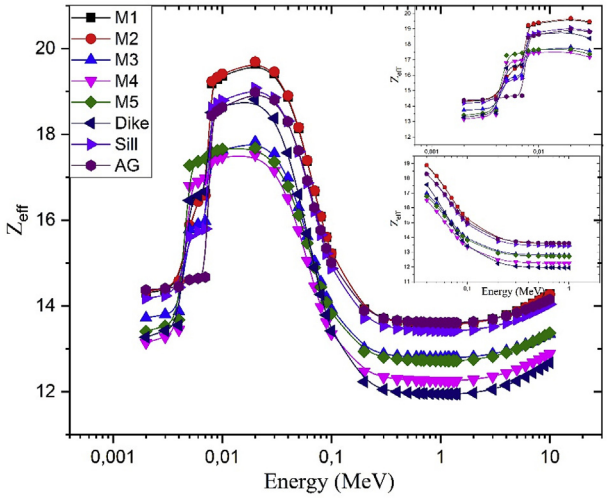

Fig. 4. The variation of Z_{eff} with incident gamma ray energy.

between 1147 and 4.16 cm^2 /g at the same energy values. Then, at intermediate gamma ray energy range between 0.03 and 1 MeV, the μ_m values for all rocks have a very slow decreasing rate with increasing the energy due to the domination of the Compton scattering mode of interaction in which ($\sigma_{comp} \propto Z$). The rock samples M2 and M1 exhibit the highest values of the μ_m and varied between 1.88 and 0.069 cm^2 /g at energy range 0.03 and 1 MeV respectively. In the other hand, the sample Dike exhibits the lowest μ_m and varied between 1.38 and 0.0633 MeV at energy range varied between 0.03 and 1 MeV respectively. Finally, in the high gamma ray energy region (i.e. E > 1 MeV) the μ_m for all selected rock samples is almost constant which is attributed to pair production cross section where ($\sigma_{pair\ pro} \propto \log E$) [7]. In this energy, the highest μ_m was observed for M2 and M1 and in the range of 0.069 and 0.0270 cm^2 /g between 1 and 10 MeV, while the lowest μ_m was observed for dike rocks and varied between 0.0633 and 0.0228 cm^2 /g along the same energy range.

Moreover, the μ_m for all selected rocks was calculated using XCOM database. The results obtained from XCOM database was compared to those simulated using MCNP 5 code. The simulated μ_m for all selected rocks was found in a good agreement with the μ_m calculated theoretically using XCOM program as shown in the supplementary information in Table S1. The difference between the simulated and computed μ_m for all selected rock samples was found to vary between 0.01 and 8%.

The mean free path (MFP) is a shielding characteristic, which describes the interaction of radiation with the shielding material atoms. The better shielding material is that exhibits a small MFP. From the simulated μ_m values, the MFP was computed for the selected rock samples. The mode in which the MFP varied with the incident gamma ray energy for the rock samples under study was plotted in Fig. 3. It is clear that the MFP for all rock samples is energy dependent.

The MFP for all selected rock samples in low energy rage ($E \leq 0.02$ MeV) is almost constant because of the photoelectric effect which is dominant in this energy region. The MFP increased gradually in intermediate and high energy range ($0.03 \leq E \leq 10$ MeV) which means that the intermediate and high energy photons can penetrate the rock samples easily. It can conclude from the curve that the lowest MFP was obtained for basalt (M1, M2 and Sill) and Rhyolite (AG) rocks, but the highest MFP obtained by limestone (M3, M4, M5 and Dike). The density of the rocks plays an important factor that affects the values of the MFP for the present rocks. From Table 1, AG, sill have the highest density values (2.57 and 2.375 g/cm^3 respectively) and this explain

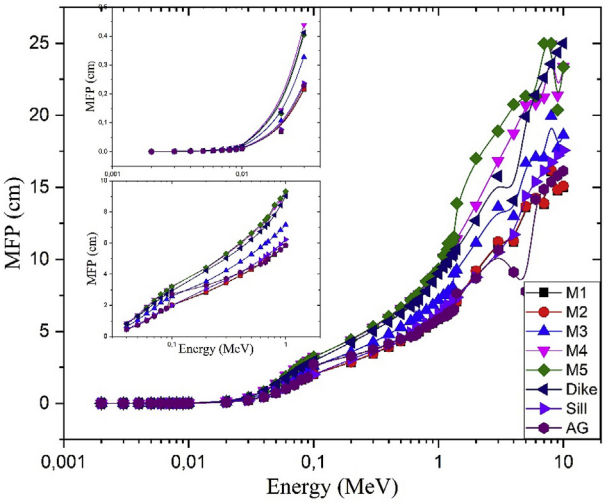

Fig. 3. The Variation of MFP with gamma ray energy.

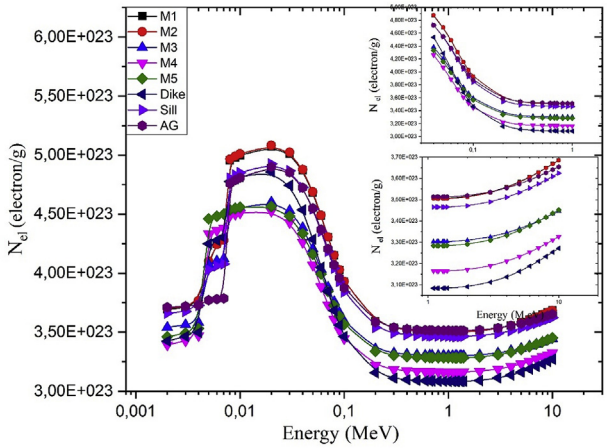

Fig. 5. The Variation of the Electron density with incident gamma ray energy.

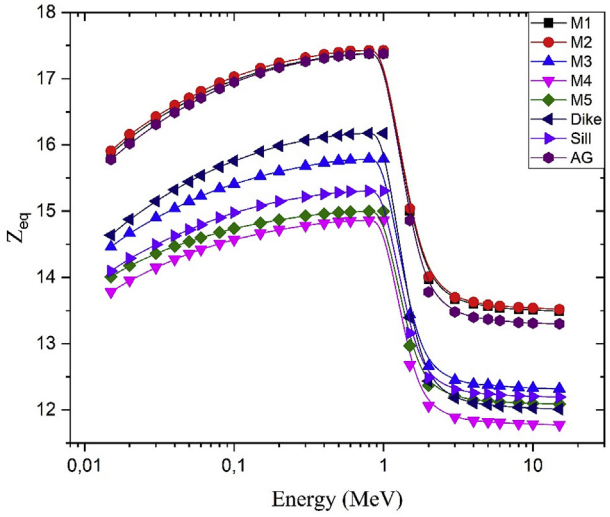

Fig. 6. Variation of Z_{eq} with incident gamma ray energy.

the low MFP values for these two rocks, while the lowest density was observed for M5 (1.6 g/cm^3) followed by dike (1.75 g/cm^3), therefore we observed the high MFP values for M5 and dike rocks.

The Z_{eff} for all selected rock samples was computed with the support of all partial interaction processes in the energy range ($0.002 \leq E \leq 10$ MeV) and illustrated in Fig. 4 It can be seen that the maximum Z_{eff} for all selected rocks was attended at gamma ray energy ($E = 0.02$ MeV) and the minimum Z_{eff} was achieved in the energy range ($0.2 \leq E \leq 8$ MeV). The highest Z_{eff} values were found for basalt rocks M1 and M2 ($Z_{eff} = 19.96$), but the lowest Z_{eff} values were obtained for dike rock ($Z_{eff} = 11.94$). The Z_{eff} increases gradually in the low energy region ($0.002 \leq E \leq 0.02$ MeV) and this is attributed to photoelectric effect. The Z_{eff} has no significant variation in the energy range ($0.008 \leq E \leq 0.03$ MeV) due to the Compton scattering effect. Finally, in the energy range ($E > 0.05$ MeV) the Z_{eff} increases rapidly.

The effective electron density N_{el} is also calculated for rock samples under study in energy range ($0.002 \leq E \leq 10$ MeV) and the results are illustrated in Fig. 5. The mode of variation of the N_{el} with the incident gamma ray photons energy was found to be similar to that of Z_{eff}.

The equivalent atomic number Z_{eq} is a parameter used in the *EBF* calculation processes and it describes the shielding properties of rock samples in terms of equivalent element. The *Zeq* is calculated from the Compton scattering only in the energy range ($0.015\ MeV < E < 15\ MeV$) and the results are plotted graphically in Fig. 6. It is clear that the Z_{eq} reaches its maximum value for all selected rock samples at gamma ray energy ($E = 1\ MeV$), but the minimum value was achieved for the energy range $E \geq 2\ MeV$. The Z_{eq} increases gradually with increasing the energy in the energy range ($0.015 < E < 1\ MeV$) due to the Compton effect process and then decrease rapidly with energy in the energy range ($E > 1 MeV$) due to pair production effect. The highest value of the Z_{eq} was observed for M1, M2 and AG samples, whereas the lowest Z_{eq} was found for M4 sample.

It is very important to make a correction for the attenuation

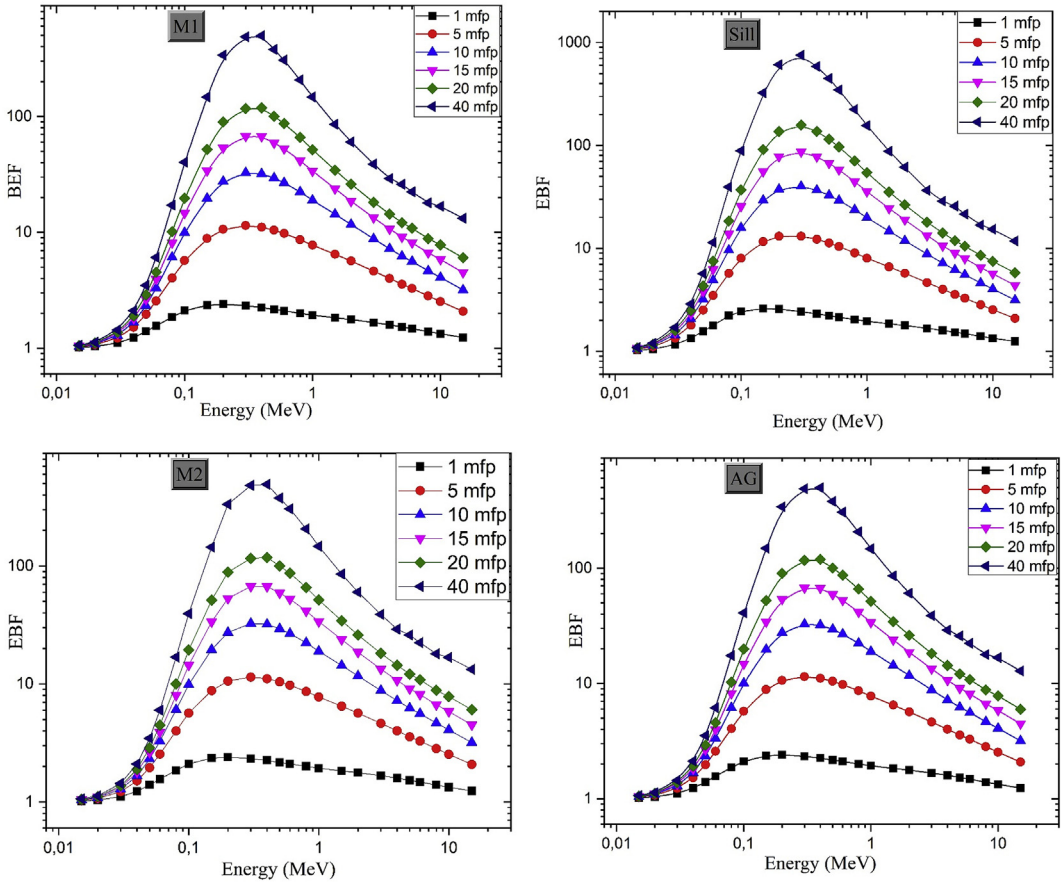

Fig. 7. The variation of buildup factor with gamma ray energy for basalt and rhyolite rocks.

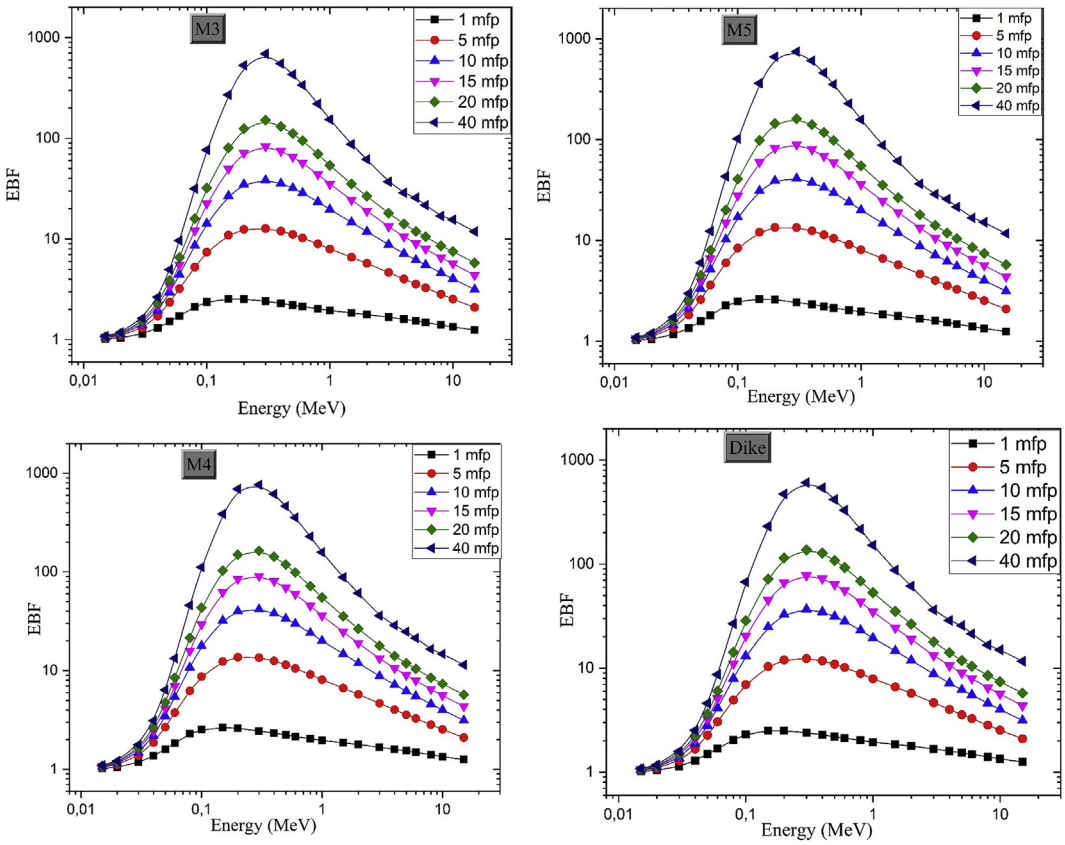

Fig. 8. The Variation of the EBF with gamma ray energy for limestone rocks.

calculation due to the effect of secondary gamma ray emission so the EBF should studied for any shielding material. The EBF for basalt and rhyolite rock samples M1, M2, Sill and AG were calculated and illustrated in Fig. 7. It is clear that the EBF values for all selected rock samples attend the maximum values at about 0.03 MeV due to the multiple scattering caused by Compton interaction, but the lowest values of the EBF achieved at the low energy due to the fast absorption of low energy photon and this didn't lead to build up for the photons [31]. From Fig. 7 we found that Sill rock sample has the highest EBF and it varied between 1.022 and 754 in the energy range between $(0.015 < E < 15$ MeV), while the lowest EBF was observed for basalt rock M2 and it varied between 1.017 and 491 in the same energy range. In term of the penetration depth, the highest EBF achieved for penetration depth 40 mfp, but the lowest EBF achieved for low penetration depth viz. 1 mfp.

The mode in which the EBF varied with the incident gamma ray energy for limestone rock samples (i.e. M3, M4, M5 and dike) was studied and illustrated in Fig. 8. It is clear that the highest EBF for limestone rocks was attended by the rock sample coded as M4 and varied between 1.024 and 764 in energy range $(0.015 < E < 15$ MeV), but the lowest EBF was obtained by dike and varied between 1.019 and 607 in the same energy range. It can be seen that the EBF for all the studied limestone rock attends to maximum at energy rage between (0.2 and 0.5 MeV) due to the domination of Compton scattering in this region. It was observed also that the EBF values for all rocks are small up to 0.06 MeV and this is due to the effect of photoelectric absorption.

4. Conclusion

The present work focused on the evaluation of the mass attenuation coefficient for eight different rock samples using MCNP5 code and XCOM database. The comparison showed agreement between the simulated and XCOM data. The highest μ_m was found for basalt rocks M1, M2 and rhyolite rock AG while the lowest μ_m was reported for dike sample. Some other parameters were also evaluated to understand the radiation shielding properties for the investigated samples. The lowest MFP was achieved by basalt rocks M1, M2 and the highest MFP achieved by limestone rocks. The Z_{eff}, and N_{el} were also studied for all selected rocks and the results showed that M1, M2 and AG possess high Z_{eff}, and N_{el} values. The EBF values for the studied rocks were also evaluated using the G-P fitting method. Basalt rocks M1, M2 and rhyolite rocks show a better shielding property than basalt sill and limestone samples.

Appendix A. Supplementary data

Supplementary data to this article can be found online at https://doi.org/10.1016/j.net.2019.05.013.

References

[1] P. Kaur, K.J. Singh, S. Thakur, P. Singh, B.S. Bajwa, Investigation of bismuth borate glass system modified with barium for structural and gamma-ray shielding properties, Spectrochim. Acta Part A Mol. Biomol. Spectrosc. 206 (2019) 367–377, https://doi.org/10.1016/j.saa.2018.08.038.
[2] H.S. Gökçe, Ç. Yalçınkaya, M. Tuyan, Optimization of reactive powder concrete by means of barite aggregate for both neutrons and gamma rays, Constr. Build. Mater. 189 (2018) 470–477, https://doi.org/10.1016/j.conbuildmat.2018.09.022.
[3] V. Beir, Health Effects of Exposure to Low Levels of Ionizing Radiation, 1990.
[4] S.S. Obaid, D.K. Gaikwad, P.P. Pawar, Determination of gamma ray shielding parameters of rocks and concrete, Radiat. Phys. Chem. 144 (2018) 356–360, https://doi.org/10.1016/j.radphyschem.2017.09.022.
[5] B. Mavi, Experimental investigation of γ-ray attenuation coefficients for

granites, Ann. Nucl. Energy 44 (2012) 22–25, https://doi.org/10.1016/j.anucene.2012.01.009.
[6] B. Pomaro, F. Gramegna, R. Cherubini, V. De Nadal, V. Salomoni, F. Faleschini, Gamma-ray shielding properties of heavyweight concrete with Electric Arc Furnace slag as aggregate: an experimental and numerical study, Constr. Build. Mater. 200 (2019) 188–197, https://doi.org/10.1016/j.conbuildmat.2018.12.098.
[7] U. Kaur, J.K. Sharma, P.S. Singh, T. Singh, Comparative studies of different concretes on the basis of some photon interaction parameters, Appl. Radiat. Isot. 70 (2012) 233–240, https://doi.org/10.1016/j.apradiso.2011.07.011.
[8] O. Agar, H.O. Tekin, M.I. Sayyed, M.E. Korkmaz, O. Culfa, C. Ertugay, Experimental investigation of photon attenuation behaviors for concretes including natural perlite mineral, Results Phys 12 (2019) 237–243, https://doi.org/10.1016/j.rinp.2018.11.053.
[9] J.M. Sharaf, H. Saleh, Gamma-ray energy buildup factor calculations and shielding effects of some Jordanian building structures, Radiat. Phys. Chem. 110 (2015) 87–95, https://doi.org/10.1016/j.radphyschem.2015.01.031.
[10] M.N. Alam, M.M.H. Miah, M.I. Chowdhury, M. Kamal, S. Ghose, R. Rahman, Attenuation coefficients of soils and some building materials of Bangladesh in the energy range 276-1332 keV, Appl. Radiat. Isot. 54 (2001) 973–976, https://doi.org/10.1016/S0969-8043(00)00354-7.
[11] M.I. Sayyed, F. Akman, A. Kumar, M.R. Kaçal, Evaluation of radioprotection properties of some selected ceramic samples, Results Phys 11 (2018) 1100–1104, https://doi.org/10.1016/j.rinp.2018.11.028.
[12] S.P.S. Vishwanath, P. Singh, M.E. Medhat, Comparative studies on shielding properties of some steel alloys using Geant4, MCNP, WinXCOM and experimental results, Radiat. Phys. Chem. 106 (2015) 255–260. https://doi.org/10.1016/j.radphyschem.2014.07.002.
[13] F. Akman, M.I. Sayyed, M.R. Kaçal, H.O. Tekin, Investigation of photon shielding performances of some selected alloys by experimental data, theoretical and MCNPX code in the energy range of 81 keV–1333 keV, J. Alloy. Comp. 772 (2019) 516–524, https://doi.org/10.1016/j.jallcom.2018.09.177.
[14] O. Agar, M.I. Sayyed, F. Akman, H.O. Tekin, M.R. Kaçal, An extensive investigation on gamma ray shielding features of Pd/Ag-based alloys, Nucl. Eng. Technol. 51 (2018) 853–859, https://doi.org/10.1016/j.net.2018.12.014.
[15] M.A. Kiani, S.J. Ahmadi, M. Outokesh, R. Adeli, H. Kiani, Study on physico-mechanical and gamma-ray shielding characteristics of new ternary nano-composites, Appl. Radiat. Isot. 143 (2019) 141–148, https://doi.org/10.1016/j.apradiso.2018.10.006.
[16] M.R. Kaçal, F. Akman, M.I. Sayyed, F. Akman, Evaluation of gamma-ray and neutron attenuation properties of some polymers, Nucl. Eng. Technol. 51 (2018) 818–824, https://doi.org/10.1016/j.net.2018.11.011.
[17] A. Sharma, M.I. Sayyed, O. Agar, H.O. Tekin, Simulation of shielding parameters for TeO2-WO3-GeO2 glasses using FLUKA code, Results Phys 13 (2019) 102199, https://doi.org/10.1016/j.rinp.2019.102199.
[18] M.I. Sayyed, Bismuth modified shielding properties of zinc boro-tellurite glasses, J. Alloy. Comp. 688 (2016) 111–117, https://doi.org/10.1016/j.jallcom.2016.07.153.
[19] D.K. Gaikwad, M.I. Sayyed, S.S. Obaid, S.A.M. Issa, P.P. Pawar, Gamma ray shielding properties of TeO2-ZnF2-As2O3-Sm2O3glasses, J. Alloy. Comp. 765 (2018) 451–458, https://doi.org/10.1016/j.jallcom.2018.06.240.
[20] P. Yasaka, N. Pattanaboonmee, H.J. Kim, P. Limkitjaroenporn, J. Kaewkhao, Gamma radiation shielding and optical properties measurements of zinc bismuth borate glasses, Ann. Nucl. Energy 68 (2014) 4–9, https://doi.org/10.1016/j.anucene.2013.12.015.
[21] P. Kaur, D. Singh, T. Singh, Gamma rays shielding and sensing application of some rare earth doped lead-alumino-phosphate glasses, Radiat. Phys. Chem. 144 (2018) 336–343, https://doi.org/10.1016/j.radphyschem.2017.09.018.
[22] N.S. Prabhu, V. Hegde, A. Wagh, M.I. Sayyed, O. Agar, S.D. Kamath, Physical, structural and optical properties of Sm 3+ doped lithium zinc alumino borate glasses, J. Non-Cryst. Solids 515 (2019) 116–124, https://doi.org/10.1016/j.jnoncrysol.2019.04.015.
[23] P. Kaur, D. Singh, T. Singh, Heavy metal oxide glasses as gamma rays shielding material, Nucl. Eng. Des. 307 (2016) 364–376, https://doi.org/10.1016/j.nucengdes.2016.07.029.
[24] N. Chanthima, J. Kaewkhao, Annals of Nuclear Energy Investigation on radiation shielding parameters of bismuth borosilicate glass from 1 keV to 100 GeV, Ann. Nucl. Energy 55 (2013) 23–28, https://doi.org/10.1016/j.anucene.2012.12.011.
[25] M.I. Sayyed, Half value layer , mean free path and exposure buildup factor for tellurite glasses with different oxide compositions, J. Alloy. Comp. (2016), https://doi.org/10.1016/j.jallcom.2016.11.318.
[26] I. Akkurt, Effective atomic and electron numbers of some steels at different energies, Ann. Nucl. Energy J. 36 (2009) 1702–1705.
[27] S.S. Obaid, M.I. Sayyed, D.K. Gaikwad, P.P. Pawar, Attenuation coe ffi cients and exposure buildup factor of some rocks for gamma ray shielding applications, Radiat. Phys. Chem. 148 (2018) 86–94, https://doi.org/10.1016/j.radphyschem.2018.02.026.
[28] M.S. El Nagdy, B.H. Ali, A.F. El Wakil, K.A. Gaber, Effect of physical parameters in measuring some poisonous and radionuclides in groundwater using ICP-OES : a case study in southwestern Sinai , Egypt, Arab J. Nucl. Sci. Appl. 49 (2016) 74–84.
[29] F. Akman, R. Durak, M.R. Kacal, F. Bezgin, Study of absorption parameters around the K edge for selected compounds of Gd, X Ray Spectrom. 45 (2016) 103–110, https://doi.org/10.1002/xrs.2676.
[30] Y. Harima, An approximation of gamma-ray buildup factors by modified geometrical progression, Nucl. Sci. Eng. 83 (1983) 299–309, https://doi.org/10.13182/NSE83-A18222.
[31] M.I. Sayyed, M.G. Dong, H.O. Tekin, G. Lakshminarayana, M.A. Mahdi, Comparative investigations of gamma and neutron radiation shielding parameters for different borate and tellurite glass systems using WinXCom program and MCNPX code, Mater. Chem. Phys. 215 (2018) 183–202, https://doi.org/10.1016/j.matchemphys.2018.04.106.
[32] S.R. Manohara, S.M. Hanagodimath, L. Gerward, Energy absorption buildup factors for thermoluminescent dosimetric materials and their tissue equivalence, Radiat. Phys. Chem. 79 (2010) 575–582, https://doi.org/10.1016/j.radphyschem.2010.01.002.
[33] ANSI/ANS-6.4.3, gamma ray attenuation coefficient and buildup factors for engineering materials, Am. Nucl. Soc. La Grange (1991).
[34] K.O.M.J. Berger, J.H. Hubbell, S.M. Seltzer, J. Chang, J.S. Coursey, R. Sukumar, D.S. Zucker, XCOM: Photon Cross Sections Database, 2010. https://dx.doi.org/10.18434/T48G6X.
[35] M.E. Medhat, Gamma-ray attenuation coefficients of some building materials available in Egypt, Ann. Nucl. Energy 36 (2009) 849–852. https://doi.org/10.1016/j.anucene.2009.02.006.
[36] C.S.Y. Elmahroug, B. Tellili, Determination of total mass attenuation coefficients, effective atomic numbers and electron densities for different shielding materials, Ann. Nucl. Energy 75 (2015) 268–274. https://doi.org/10.1016/j.anucene.2014.08.015.
[37] S.A.M. Issa, A.M.A. Mostafa, T.A. Hanafy, M. Dong, X. Xue, Comparison study of photon attenuation characteristics of Poly vinyl alcohol (PVA) doped with Pb(NO 3) 2 by MCNP5 code, XCOM and experimental results, Prog. Nucl. Energy 111 (2019) 15–23, https://doi.org/10.1016/j.pnucene.2018.10.018.
[38] A.H. Abdalsalam, M.I. Sayyed, T. Ali Hussein, E. Şakar, M.H.A. Mhareb, B. Ceviz Şakar, B. Alim, K.M. Kaky, A study of gamma attenuation property of UHMWPE/Bi 2 O 3 nanocomposites, Chem. Phys. 523 (2019) 92–98, https://doi.org/10.1016/j.chemphys.2019.04.013.
[39] M.G. Dong, M.I. Sayyed, G. Lakshminarayana, M. Çelikbilek Ersundu, A.E. Ersundu, P. Nayar, M.A. Mahdi, Investigation of gamma radiation shielding properties of lithium zinc bismuth borate glasses using XCOM program and MCNP5 code, J. Non-Cryst. Solids 468 (2017) 12–16, https://doi.org/10.1016/j.jnoncrysol.2017.04.018.
[40] M.I. Sayyed, H.O. Tekin, O. Kılıcoglu, O. Agar, M.H.M. Zaid, Shielding features of concrete types containing sepiolite mineral: comprehensive study on experimental, XCOM and MCNPX results, Results Phys 11 (2018) 40–45, https://doi.org/10.1016/j.rinp.2018.08.029.
[41] B. Oto, N. Yildiz, F. Akdemir, E. Kavaz, Investigation of gamma radiation shielding properties of various ores, Prog. Nucl. Energy 85 (2015) 391–403, https://doi.org/10.1016/j.pnucene.2015.07.016.